

Structural Flexibility Identification by Processing Dynamic Macro Strain Measurements

S.L. Guo , Q. Xia, and J. Zhang ¹⁾

*International Institute for Urban Systems Engineering, Southeast University, Nanjing
210096, China*

¹⁾ jianzhang.civil@gmail.com

ABSTRACT

In contrast to traditional modal identification methods processing structural accelerations for modal parameter identification, a multiple reference impact testing method using long-gauge fiber optical sensors and the related data processing approach are proposed. First, macro strains of key structural elements during the impact testing are measured through long-gauge fiber optic sensors, which subsequently are used to estimate the strain frequency response functions (FRFs) of the structure. Second, a method is proposed to estimate strain mode shapes from the strain FRFs, and corresponding displacement mode shapes are calculated by applying an improved conjugate beam method. Finally, the strain flexibility character of the structure is identified by using the identified strain and displacement mode shapes with normalization. The advantage of long-gauge fiber optic sensors measuring averaged strains in a long length (e.g., 1 meter) provides the opportunity for strain modal analysis. The output of the proposed method, strain flexibility, is meaningful for static strain prediction and structural capacity evaluation. Examples investigated successfully verified the effectiveness of the proposed method for structural strain flexibility identification.

Key words: long-gauge FBG sensors, dynamic macro strain, strain modal analysis, strain flexibility identification.

1. INTRODUCTION

Various kinds of Structural Health Monitoring (SHM) approaches have been developed for the assessment and management of civil infrastructures, such as static load test, ambient vibration test, and impact test (Adewuyi and Wu 2011; Hsu et al. 2011). As limited available funds, infrastructure owners, operators and managers are being forced to optimize their available resources to further the state-of-the-art in diagnostics and prognostics for civil infrastructure systems. Ambient vibration test has been widely used as a basis for an evaluation of infrastructure condition. It measures the structural response under ambient excitations such as traffic, wind, temperature and other ambient forces, thus, it is easy to perform, especially for large-scale structures

¹⁾ Professor

which are difficult to excite by human-made forces (Carden and Brownjohn 2008; Zhang et al. 2009). A great number of case studies based on ambient tests of actual bridges have been carried out in the literature, e.g., the Golden Gate Bridge, the Z20-bridge, the Kap Shui Mun Bridge, the Hakucho Bridge, the Humber Suspension Bridge, and the Throgs Neck Bridge (Pakzad and Fenves 2009; Ko et al. 2002; Siringoringo and Fujino 2008; Brownjohn et al. 2009; Peeters and Roeck 2001; Zhang et al. 2009). Processing ambient vibration data is able to output structural modal parameters such as frequency, damping and mode shapes through various modal identification methods (James et al. 1995; Weng et al. 2008; Sohn et al. 2004; Catbas et al. 2004). However, it is still far from meeting the structure owners' expectations because they generally intend to know much more detailed information about the investigated structure, for instance, the stiffness distribution and damage conditions.

Compared to the ambient vibration test which only identifies structural modal parameters, the Multi-Reference Impact Testing (MRIT), which utilizes hammer/shaker hitting at a single or multiple points to excite the structure and measuring both the input impacting forces and the corresponding structural acceleration responses at selected positions, is able to extract much more detailed structural modal parameters sufficient for identifying the structural flexibility, from which the structural deflection under any static load can be successfully predicted. Namely, the impacting test has the assets to output both dynamic (frequencies and mode shapes) and static (flexibility) characteristics. Case studies of several short/middle span bridges have illustrated that the predicted deflections from the MRIT data were comparable with those from the truck static load test. Thus, the identification of the flexibility from impact testing is promising. Though, the drawback of the traditional MRIT is that it only identify flexibility from accelerations for deflection prediction, while the bridge maintenance codes generally require both deflection and strain information for capacity evaluation (AASHTO 2003 Guide Manual for Condition Evaluation and LRFR of Highway Bridges). It will be perfect if the strain flexibility feature of the structure can also be identified during the impact testing through the strain modal analyses.

The theory of strain modal analysis has been developed for a long time (Adewuyi and Wu 2011; Li and Wu 2005, 2006, 2007). Yam et al. (1996) have found that the strain mode shapes are more sensitive to structural local changes than the displacement mode shapes. However, traditional foil strain gauges are not suitable for large-scale civil SHM not only because of the problem of stability, durability and long-term reliability but also for the reason that they are basically 'point' sensors. It may therefore be too impractical to deploy sensors to all elements and components considered possibly critical. Moreover, strain measurements from traditional point sensors reflect structural local, not global, information. Thus, detecting strain mode shapes using conventional sensors is challenging. With the recent advances in sensors and sensing technology, measurement equipment and signal processing techniques, structural dynamic properties can be measured more accurately and reliably. Specifically, long-gauge Fiber Bragg Grating (FBG) optic sensors are more promising sensing alternatives for civil SHM systems which were used for monitoring the strain responses of the structure. Vast literature on the development of optic FBG distributed strain sensors, and their applications in SHM of civil infrastructure systems can be found in Sohnet et al. (2003), Ansari (1997), Inaudi (2001), Schulz et al. (2001), and Casas and Cruz (2003). Some

basic advantages of FBG include flexibility, embed ability, multiplicity, immunity to electro-magnetic interference. Especially, Wu et al. (2006, 2011) developed a long-gauge FBG sensor, which has the unique feature to measure the averaged strain over arbitrary gauge lengths. The dynamic strain output through this novel sensor not only reflect local, but also global structural information by designing a long-gauge of the sensor, for instance, 1~2 meters.

Given the motivation and background presented previously, in this article, a new method to identify structural strain flexibility from the multiple reference impact test data with a novel long gauge FBG sensor is proposed. Firstly, distributed strain measurements are outputted through long-gauge optic FBG sensors during the impact test, and subsequently the strain FRFs are estimated from the MRIT measurements. Second, a method is proposed to identify strain mode shapes based on the feature of the estimated strain FRFs, then displacement mode shapes are calculated from the strain mode shapes through an improved conjugate beam approach. Finally, relying on long gauge strain mode shapes and displacement mode shapes, the structural strain flexibility are identified. The merit of the proposed method is that (1) the long-gauge FBG sensor is used for macro strain measurement, which is more appropriate for strain modal analyses than that from point strain gauges; (2) the multiple reference impact test method is employed to output accurate strain FRFs, and (3) the method to identify strain mode shapes, displacement mode shapes and strain flexibility has been proposed by processing the macro strain time histories.

2. Long-gauge FBG sensors and theory for strain flexibility identification

2.1 Distributed strain measurements with long gauge FBG Sensors

The technology of distributed strain sensing is greatly required in engineering practices of civil infrastructure monitoring and maintenance. Fiber Bragg Grating (FBG) sensors are gaining increasing attention because it provides many advantages compared to the metal foil strain gages, for instance, light weight and high precision. An long-gauge fiber optic sensor has been developed by the authors based on the advantage of the FBG technology (Li and Wu 2007; Wu and Zhang 2011). Other than the merit of high spatial resolution, the developed sensor was designed to have a long gauge, thus it is able to measure the average strain within the gauge length. To avoid unsustainable costs for the sensors, the concept of salient area monitoring has been developed, which installs long gauge FBG sensors in key regions of an engineering structure and connects sensors in series to make an FBG sensor array for area macro-strain measuring. In this way, the measurement of distributed strain sensing scheme will be implemented for an accurate and effective strain monitoring in civil engineering structures.

Although the obvious potentials of FBG sensors for SHM, their practical applications to civil engineering structures still face some primary technological challenges due to the fragility of bare fiber whose coat has to be removed from commercial optical fiber to fabricate FBG with high sensitivity. Moreover, appropriate methods for FBG sensor packaging and bonding with host structures should be carefully considered to protect the brittle fiber from harsh environment and ensure measurements of interest to transfer fully from object structure to sensors. In addition, the traditional problem that exists in

most of fiber optic sensors of cross-sensitivity between strain and temperature needs to be resolved as well. To solve the above-mentioned problems, a new packing design for long gauge-FBG sensors has been developed (Li and Wu 2005, 2006, 2007). The manufacture process of the developed long-gauge sensor is illustrated in following steps as: (a) A steel tube of 2 mm diameter and gauge length is used instead of the aforementioned hollow composite device for sleeved FBG; (b) The optical fiber is first fixed onto one end of the tube, via pretension applied to its free part by using suspended weights and then onto the other end of the tube. This manner ensures that the sleeved FBG can work together with the tube and compressive measurements can be effectively obtained; (c) The optical fiber outside of the tube is then connected with SMC using a fusion machine; (d) Carbon fiber tow is utilized to sandwich the above mechanism. It is worth stressing that the length of tow should be ensured to cover the fusion area with SMC as the optical fiber in this part has to be removed of the coat for fusion and hence is very fragile; (e) Epoxy resin is pasted onto the sandwich structure including carbon fiber tow and in-tube FBG. After epoxy hardening, they are composed to an integrated solid and can work together.

By designing the FBG sensor with a long gauge and fixing its two ends (Fig. 1(a)), the in-tube fiber has the same mechanical behavior and hence the strain transferred from the shift of Bragg centre wavelength represents the average strain (or macro-strain) over the sensor gauge length. An improved packaging design has also been proposed to enhance the measuring sensitivity and temperature compensation of LG-FBG sensors by utilizing two materials with different modulus to package the optic fiber and to impose deformation within the gauge length, largely on the essential sensing part of the FBG (Fig. 1(b)). Due to its long gauge length, the developed LG-FBG strain-sensing technique is capable to implement effectively the combination of both global and local measurements in order to detect structural damage in civil constructions, (Fig. 1(c)).

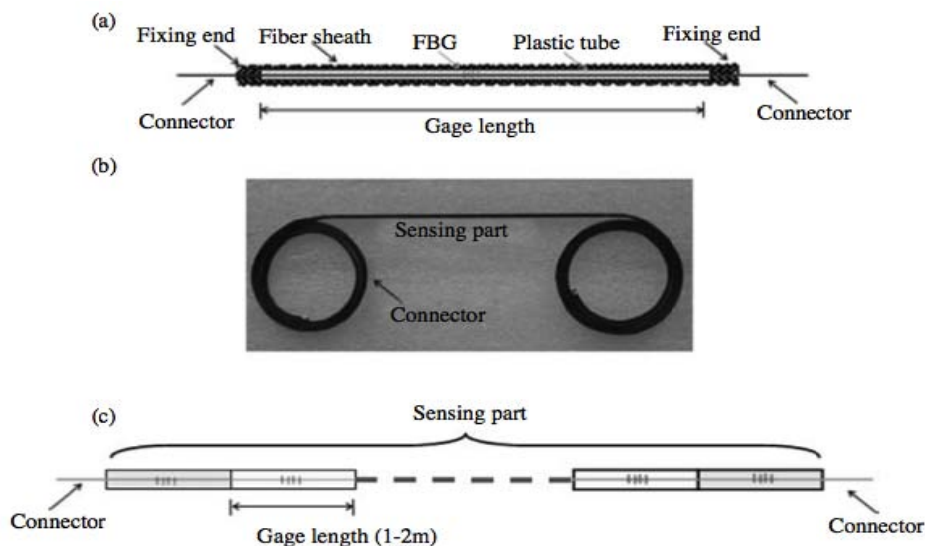


Fig. 1 Packaged LG-FBG sensor: (a) schematic picture; (b) actual sensor; (c) sensor arrays

2.2 Theory development for strain flexibility identification

The multiple reference impact test method with the long-gauge sensor is proposed, which simultaneously measure the impact force and strain data. The methods to process the impact force and accelerations are available in the literature. In this section, the theory to deal with the impacting force and macro strain data from the MRIT are developed for strain modal analyses and strain flexibility identification.

2.2.1 Strain FRFs

The displacement FRF of point p due to the force applied in q is defined by:

$$H_d^{pq}(\omega) = \sum_{r=1}^N \frac{\phi_{pr} \phi_{qr}}{M_r(\omega_r^2 - \omega^2 + 2j\xi_r\omega_r\omega)} \quad (1)$$

where $\omega_r = \sqrt{\frac{K_r}{M_r}}$ is the r -th modal circular frequency of the structure, K_r and M_r are modal stiffness and modal mass respectively, $\xi_r = \frac{C_r}{2M_r\omega_r}$ is the structural r -th modal damping ratio, and ϕ is structural mode shape.

In a general beam as shown in Fig. 2, each node contains two DOFs (vertical displacement and rotation). Under the condition of single-load excitation, the long gauge strain measurement in substructure m is:

$$\varepsilon_m(\omega) = \mu_m[\theta_o(\omega) - \theta_p(\omega)] \quad (2)$$

Where $\mu_m = \frac{h_m}{L_m}$, h_m is the distance from the sensor to the neutral axis of the beam while θ_o and θ_p are the rotation of each DOF.

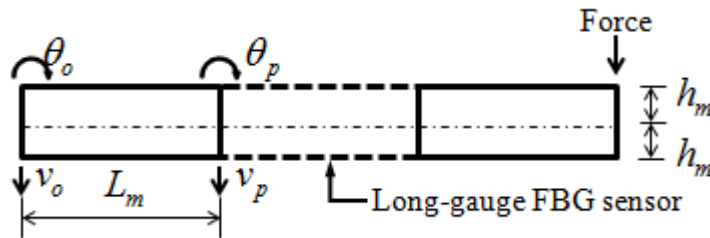


Fig. 2 Relation between rotation and macro-strain

The long gauge strain FRF of the element m is:

$$H_{\varepsilon}^{mq}(\omega) = \mu_m \frac{[v_o(\omega) - v_p(\omega)]}{f_q(\omega)} = \mu_m [H_d^{oq}(\omega) - H_d^{pq}(\omega)] \quad (3)$$

$H_d^{oq}(\omega)$ corresponds to the angular displacement FRF of the node o . Therefore, it is derived that

$$H_{\varepsilon}^{mq}(\omega) = \sum_{r=1}^N \frac{\mu_m(\phi_{or} - \phi_{pr})\phi_{qr}^v}{M_r(\omega_r^2 - \omega^2 + 2j\xi_r\omega_r\omega)} \quad (4)$$

The above equation is derived to be below by defining $\phi_{\varepsilon}^{mr} = \mu_m(\phi_{or} - \phi_{pr})$ which indicates the long gauge strain mode shape,

$$H_{\varepsilon}^{mq}(\omega) = \sum_{r=1}^N \frac{\phi_{\varepsilon}^{mr} \phi_{qr}^v}{M_r(\omega_r^2 - \omega^2 + 2j\xi_r\omega_r\omega)} \quad (5)$$

the equation above represents long-gauge strain FRF which incorporates the mass, stiffness and damping ratio of the structure and how it responds to a known input to the system. Thus it can be used to estimate structural strain modal parameters.

2.2.2 The proposed strain modal analysis method

By comparing Eqs. (1) and (5), it is found that there are mainly two differences between strain FRF matrix and displacement FRF matrix: (a) the strain FRF matrix is an asymmetric matrix; (b) in the strain FRF matrix, each column reflects the modal strain information of the structure, whereas each row represents the modal displacement information. Similar to Eq. (5), the strain FRF of the element q strain response under the force excitation at the node m is $H_{\bar{\varepsilon}}^{qm}(\omega) = \sum_{r=1}^N \frac{\phi_{\bar{\varepsilon}}^{qr} \phi_v^{mr}}{M_r(\omega_r^2 - \omega^2 + 2j\xi_r \omega_r \omega)}$. Since we have $\phi_{\bar{\varepsilon}}^{mr} \phi_v^{qr} \neq \phi_{\bar{\varepsilon}}^{qr} \phi_v^{mr}$, so $H_{\bar{\varepsilon}}^{qm}(\omega) \neq H_{\bar{\varepsilon}}^{mq}(\omega)$ namely the strain FRF matrix is an asymmetric matrix.

Secondly, the value of r -th component of strain FRF matrix in ω_r is $H_{\bar{\varepsilon}}^{mq}(\omega_r) = \frac{\phi_{\bar{\varepsilon}}^{mr} \phi_v^{qr}}{2j\xi_r M_r \omega_r^2}$. For ${}_r H_{\bar{\varepsilon}}^{mq}(\omega_r)$, extending a column at same order of frequency ω_r , we have ${}_r H_{\bar{\varepsilon}}^{:q}(\omega_r) = \{\phi_{\bar{\varepsilon}}^r\} \frac{\phi_{qr}}{2j\xi_r M_r \omega_r^2}$, where $\{\phi_{\bar{\varepsilon}}^r\}$ indicates the r -th punctual strain mode shapes, and the coefficient $\frac{\phi_{qr}}{2j\xi_r M_r \omega_r^2}$ is a constant relative to the r -th frequency and mode shape, so at the r -th frequency ω_r , we can suppose that $H_{\bar{\varepsilon}}^{:q}(\omega_r) \approx {}_r H_{\bar{\varepsilon}}^{:q}(\omega_r)$, which means that any member of the strain FRF matrix represents structural modal information.

Similarity, For ${}_r H_{\bar{\varepsilon}}^{mq}(\omega_r)$, extending a row at same order of frequency ω_r , we have ${}_r H_{\bar{\varepsilon}}^{m:}(\omega_r) = \{\phi_r\}^T \frac{\phi_{\bar{\varepsilon}}^{mr}}{2j\xi_r M_r \omega_r^2}$, where $\{\phi_r\}^T$ is the r -th vertical displacement mode shape and the coefficient $\frac{\phi_{\bar{\varepsilon}}^{mr}}{2j\xi_r M_r \omega_r^2}$ is a constant relative to the r -th frequency and mode shape, so at the r -th frequency ω_r , we can suppose that $H_{\bar{\varepsilon}}^{m:}(\omega_r) \approx {}_r H_{\bar{\varepsilon}}^{m:}(\omega_r)$, which means that any member of the strain FRF matrix represents structural vertical displacement information. The feature of the strain FRF described above is easily seen from the following equation:

$$\begin{array}{c}
 q\text{-th column} \\
 \downarrow \\
 [H^{\varepsilon}(\omega)] = \left[\begin{array}{cccc}
 \sum_{r=1}^n \phi_{1r}^{\varepsilon} \frac{\phi_{qr}^v}{C_r(\omega)} & & & \\
 & \vdots & & \\
 \sum_{r=1}^n \frac{\phi_{pr}^{\varepsilon}}{C_r(\omega)} \phi_{1r}^v & \cdots & \sum_{r=1}^n \phi_{pr}^{\varepsilon} \frac{1}{C_r(\omega)} \phi_{qr}^v & \cdots & \sum_{r=1}^n \frac{\phi_{pr}^{\varepsilon}}{C_r(\omega)} \phi_{N_j r}^v \\
 & & \vdots & & \\
 \sum_{r=1}^n \phi_{N_s r}^{\varepsilon} \frac{\phi_{qr}^v}{C_r(\omega)} & & & &
 \end{array} \right] \leftarrow p\text{-th row} \quad (6)
 \end{array}$$

where: N_j and N_s represent respectively the number of displacement mode shapes and strain mode shapes of all nodes and $C_r(\omega) = M_r(\omega_r^2 - \omega^2 + 2j\xi_r \omega_r \omega)$. In brief, based on this feature, strain mode shapes is proposed to be identified by picking the peaks of the FRFs in column as shown in Fig. (3). Similarly, displacement mode shapes can be identified from the strain FRFs in a row.

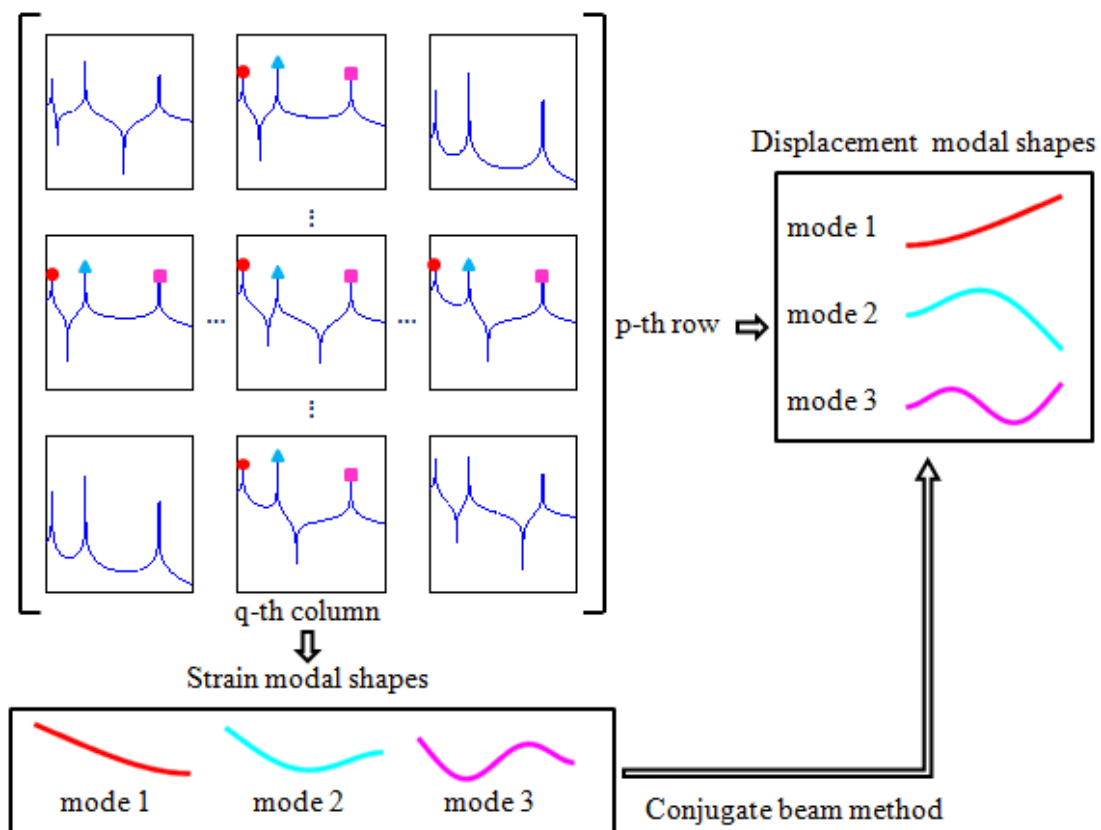


Fig. 3 Strain modal parameter identification based on the strain FRF features

2.2.3 The improved conjugate beam approach for displacement mode shape estimation

Displacement mode shapes can be estimated directly from the strain FRF as presented above, however it requires a row of the FRF elements. It means that all nodes need be impacted during the multiple reference impact test, which significantly increase the experiment cost. An improved conjugate beam approach is used to calculate displacement mode shape from the estimated strain mode shape.

According to the conjugate beam theory, the bending moment distribution $M(x)$ on the real beam is considered as load distribution $\bar{q}(x)$ on the conjugate beam, then its corresponding bending moment distribution $\bar{M}(x)$ is equivalent to real beam's vertical displacement distribution $y(x)$, namely: $y(x) = \frac{\bar{M}(x)}{EI}$. Hereafter, the symbol $\bar{\quad}$ indicates that the parameter concerned is referred to the conjugate beam. For the Euler-type beam, the relationships between its deformation $\varepsilon(x)$, curvature $\kappa(x)$ and bending moment $M(x)$ are linear as shown below:

$$\kappa(x) = \frac{\varepsilon(x)}{z} = \frac{M(x)}{EI} \quad (7)$$

thus:

$$M(x) = EI \frac{\varepsilon(x)}{z} \quad (8)$$

where z is the distance from the beam's surface to the neutral axis.

Assuming that the conjugate beam's load distribution is equal to $\bar{q} = \frac{\varepsilon(x)}{z}$, we can conclude that the corresponding bending moment distribution $\bar{M}(x)$ of the conjugate beam is exactly identical to the real beam's vertical displacement distribution $y(x)$.

The improved conjugate beam method is based on the discretization of real beam's long gauge measurements. The nodal vertical displacement of the real beam is calculated by its long gauge strain measured from FBG sensors. Since the FBG sensors measure the long gauge macroscopic strains which are different from the traditional punctual strains, moreover, they measure the average strains within the gauge length, so precessing with the discretization of the continuous problem, it is possible to evaluate the nodal displacements.

Due to the fact that a simply supported beam's corresponding conjugate beam is itself, so the elementary long gauge strain of the real beam and the corresponding load distribution on conjugate beam is shown in Fig. as follow:

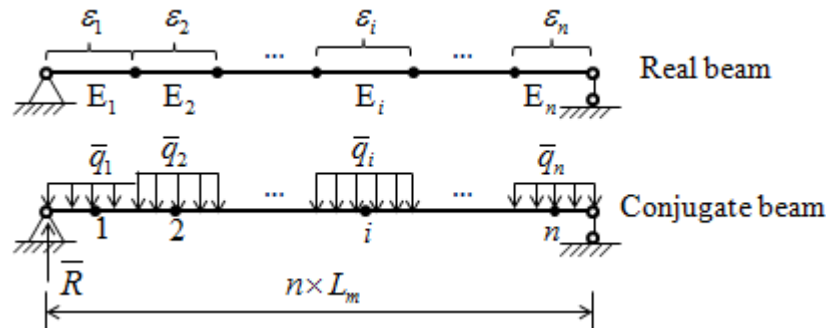


Fig. 4 Scheme of conjugate beam theory for simply supported beam

for the equilibrium, the reaction at the left support of the conjugate beam is:

$$\bar{R} = \frac{L_m}{n} \sum_{i=1}^n \bar{q}_i (n - i + 0.5) \quad (9)$$

where $\bar{q}_i = \frac{\varepsilon_i}{z}$, thus the bending moment of midpoint in each element of conjugate beam (i.e. the vertical displacement of the same point in the real beam) is:

$$y_i = L_m^2 \sum_{j=1}^i \bar{q}_j (i - j) + \bar{q}_i L_m^2 / 8 - \bar{R} L_m (i - 0.5) \quad (i = 1, 2, \dots, n) \quad (10)$$

Whereas in the case of a cantilever beam, the bending moment of midpoint in each element of conjugate beam is:

$$y_i = L_m^2 \sum_{j=1}^i \bar{q}_j (i - j) + \bar{q}_i L_m^2 / 8 \quad (i = 1, 2, \dots, n) \quad (11)$$

when we consider the measurement of long gauge strain of an element ε_i as its strain mode shape ϕ_i^ε , the vertical displacement mode shape in the middle joint of the element ϕ_i^y can be estimated by the improved conjugate beam theory.

2.2.4 Structural strain flexibility identification with known mass

The structural displacement in terms of modal coordinates can be written as follow:

$$\{U\} = [\Phi] \{Y\} \quad (12)$$

$$(-\omega^2 [m_r] + j\omega [c_r] + [k_r]) \{Y\} = [\Phi]^T \{F\} \quad (13)$$

where $[m_r]$, $[c_r]$ and $[k_r]$ are respectively system mass matrix, damping ratio and stiffness matrices expressed in natural coordinates. Solving Eq. (13), we have:

$$\{Y\} = [\varrho_r] [\Phi]^T \{F\} \quad (14)$$

therefore, in physical coordinates system is:

$$\{U\} = [\Phi][\alpha_r][\Phi]^T\{F\} \quad (15)$$

where $[\alpha_r] = \text{diag}[\alpha_1, \alpha_2, \alpha_3, \dots, \alpha_N]$, $\alpha_r = (-\omega^2 m_r + j\omega c_r + k_r)^{-1}$.

From the following relationship between strain and displacement:

$$\{\varepsilon\} = \frac{\partial^2\{U\}}{\partial x^2} z \quad (16)$$

where z is the distance from the test point and neutral axis of the beam.

By substituting Eq. (15) into Eq. (16), we have:

$$\{\varepsilon\} = \frac{\partial^2([\Phi][\alpha_r][\Phi]^T\{F\})}{\partial x^2} z \quad (17)$$

where $\{\phi\}^T[F]$ represents the energy gained by the structure from outside. Considering it as constant during differential operation, for a constant section beam, by Eq. (17), we can obtain:

$$\{\varepsilon\} = \frac{\partial^2[\Phi]}{\partial x^2} z [\alpha_r][\Phi]^T\{F\} \quad (18)$$

where $[\Phi]$ is the displacement mode shapes of the structure, making $\frac{\partial^2[\Phi]}{\partial x^2} z = [\Phi^\varepsilon]$, as $\{\Phi^\varepsilon\}$ is the structural strain mode shape. By Eq. (18), we have:

$$\{\varepsilon\} = [\Phi^\varepsilon][\alpha_r][\Phi]^T\{F\} \quad (19)$$

so the strain flexibility matrix is:

$$[f_\varepsilon] = \frac{\{\varepsilon\}}{\{F\}} = [\Phi^\varepsilon][\alpha_r][\Phi]^T = \frac{\sum_{r=1}^m \{\Phi_r^\varepsilon\}\{\Phi_r\}^T}{\omega_r^2} \quad (20)$$

where $\{\Phi^\varepsilon\}$ is the structural strain mode shapes, as we can see from the above equation that the strain flexibility matrix is asymmetry and it is important to note that for the identification of strain flexibility $[f_\varepsilon]$, the displacement vector Φ_r and strain mode shapes vector Φ_r^ε need to be normalized as mentioned following:

The k -th strain mode shape $\{\phi_k^\varepsilon\}$ obtained by strain modal analysis can be processed through the conjugate beam theory for the identification of k -th vertical displacement mode shape in midpoint of the element $\{\phi_k^v\}$. The normalization factor of the vertical displacement mode shape is:

$$a_k = \sqrt{\{\phi_k^v\}^T [M] \{\phi_k^v\}} \quad (21)$$

thus, the normalized-vertical displacement mode shape is:

$$\{\bar{\phi}_k^v\} = \frac{\{\phi_k^v\}}{a_k} \quad (22)$$

owing to the linear relationship between strain mode shape and vertical displacement mode shape, the strain mode shape has the same normalization factor as the vertical displacement mode shape, so the normalized strain mode shape is:

$$\{\bar{\phi}_k^\varepsilon\} = \{\phi_k^\varepsilon\}/a_k \quad (23)$$

where the symbol $\bar{\quad}$ indicates normalized parameter.

After calculating the structural strain flexibility, the static strain can be predicted multiplying it by static load vector acting on the structure. The static strain represents an important index in SHM practices for short/middle span bridges. A chart flow was reported to better clarify the steps followed by numerical examples studied in section 3 for static strain identification as shown in Fig. 5:

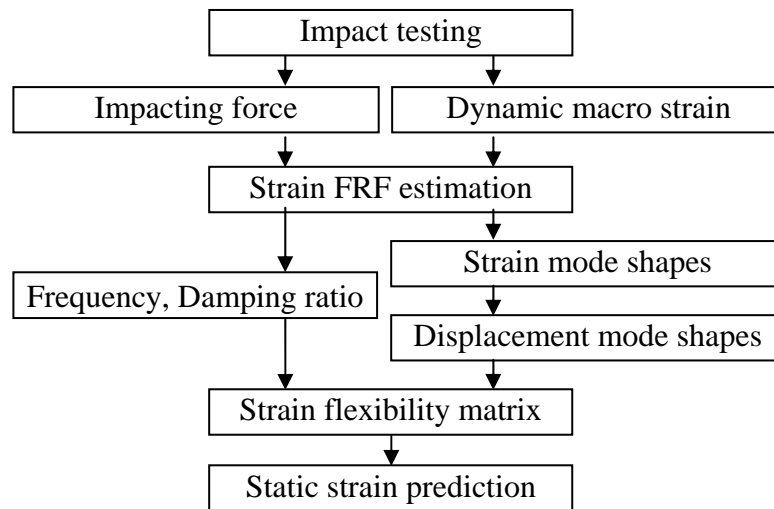


Fig. 5 Flow Chart of strain flexibility identification

3. Cantilever beam example

To verify the validity of the proposed method for the structural strain flexibility investigation, a cantilever beam as shown in Fig. 6 is first investigated. The length of the beam is 1.6 m with a cross section of 80×5 mm, the Young's modulus $E = 206 \text{ GPa}$, density $\rho = 7697 \text{ kg/m}^3$ and Poisson's coefficient $\nu = 0.3$. Eight long-gauge FBG sensors are employed on this beam as shown in Fig. 6, and the gauge of each sensor has a length of 0.2 m. Applying the impacting force at nodes 3, 5, 8, respectively, the time history of long gauge strain responses are simulated by the *Sap2000* software. 10% white noise is added into the impacting force and dynamic strain data to simulate observation noise. A typical impacting force and corresponding strain curve are plotted in Fig. 7 for illustration purpose.

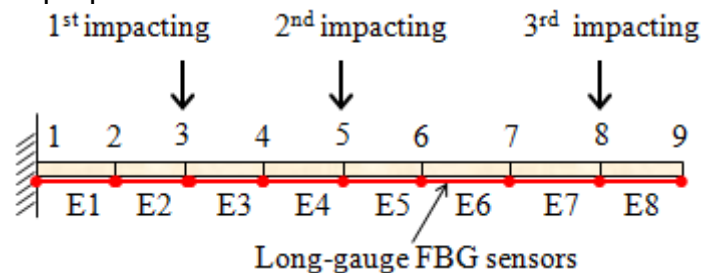


Fig. 6 Outline of cantilever beam in FEM

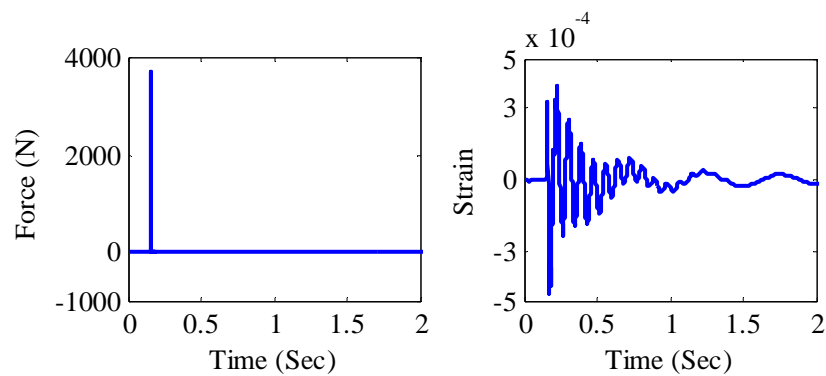


Fig. 7 Typical impact force and strain curve

Data pre-processing techniques including the filtering and averaging are used to improve the quality of the data. Then the auto/cross power spectra are calculated by using the impact force and the macro strain time histories. The strain FRFs are estimated using the H1 algorithm, which is an appropriate FRF estimation method by minimizing the noise in the output data. The application of the impacting forces at 3 reference nodes and the corresponding output of long gauge strain responses at 8 elements imply that the obtained FRF matrix's size is 8 by 3. In addition, The long gauge strain FRFs of 8 element with the impacting force on the node 3 are illustrated in Fig. 8. It is seen that the abscissas of the circles in the diagrams indicate the natural frequencies. The estimated natural frequencies of the first three modes are respectively 1.944 Hz, 11.848 Hz and 32.682 Hz, while those from the modal analysis in the *Sap2000* software are 1.926 Hz, 11.861 Hz and 32.697 Hz respectively. By picking the peaks of the FRF elements in a column in each mode, the strain mode shapes are estimated as presented in the second section. The estimated strain mode shapes in the first three modes are plotted in Fig. 9(a). The agreement between the estimated mode shapes and the exact values from the finite element analysis plotted in the same figure illustrate the accuracy of the strain mode shape identification.

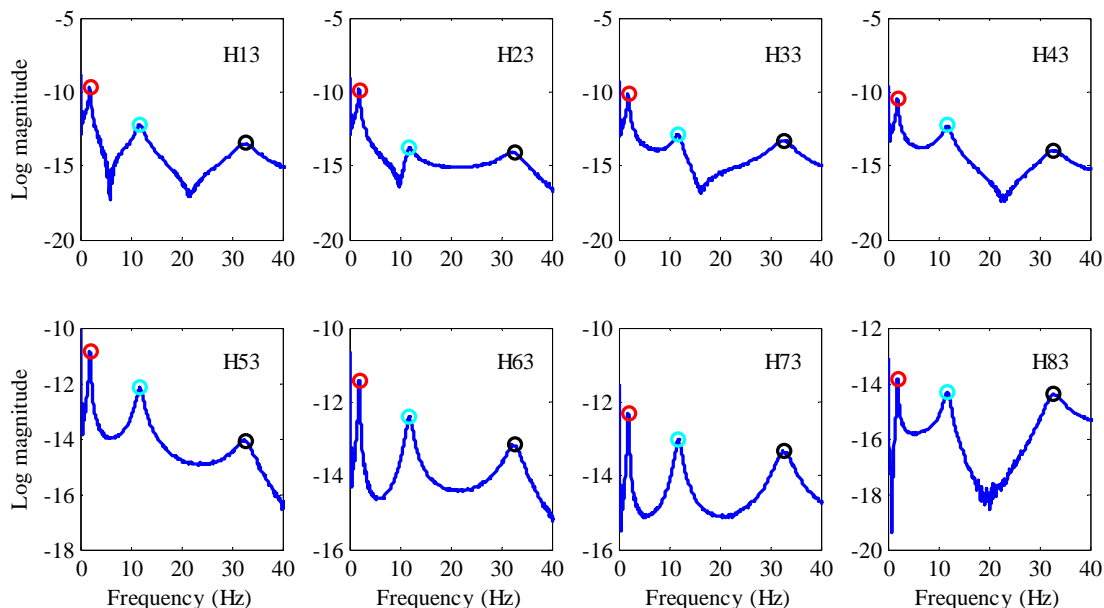


Fig. 8 The typical strain FRFs of the cantilever beam

Furthermore, the improved conjugate beam method is employed to estimate the vertical displacement mode shapes from the identified strain mode shapes. Comparative assessments between them and the exact values from the finite element analysis are illustrated in Fig. 9(b). It is necessary to point out that the red circles indicate the identified vertical displacement in middle joint of each segment and the blue lines show the FEM-based results of vertical displacement mode shapes in the middle point of each element. As perfect overlaps can be seen between two lines, it can be confirmed that values obtained by two methods are consistent.

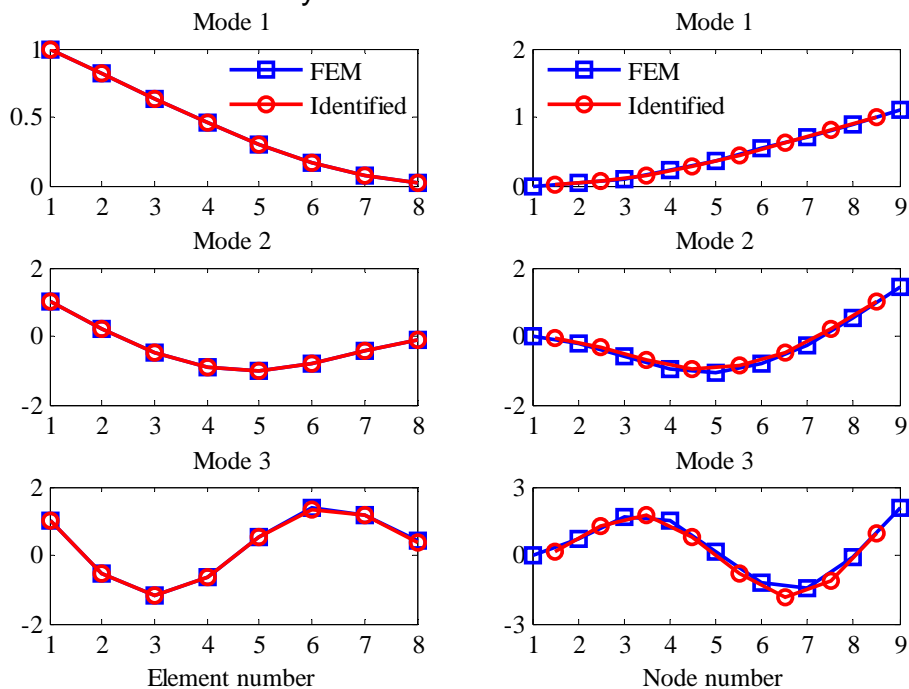


Fig. 9 Identified modal parameters, (a) strain mode shapes; (b) vertical displacement mode shapes

By assuming the mass matrix of the structure can be calculated by using structural material and geometrical parameters, the identified strain mode shapes and displacement mode shapes are normalized by Eqs. (22) and (23), then they are used to estimate structural strain flexibility through Eq. (20). The identified strain flexibility matrix of the cantilever beam is plotted in 오류! 참조 원본을 찾을 수 없습니다.10. It should be noted that during the strain flexibility identification, all displacement mode shapes are referred to middle joint's values, thus each element of the strain flexibility matrix, f_{ij}^{ε} , indicates the long gauge strain value on the element i due to the force applied on the node j . It is seen from Fig. 10 that the strain flexibility matrix of the cantilever beam is obtained by the intersection between a horizontal plane and a inclined one. The horizontal plane indicates strain flexibility values are null for free edges while the inclined one represents a linear relation among the curvatures of the elements and the corresponding positions of impacting forces.

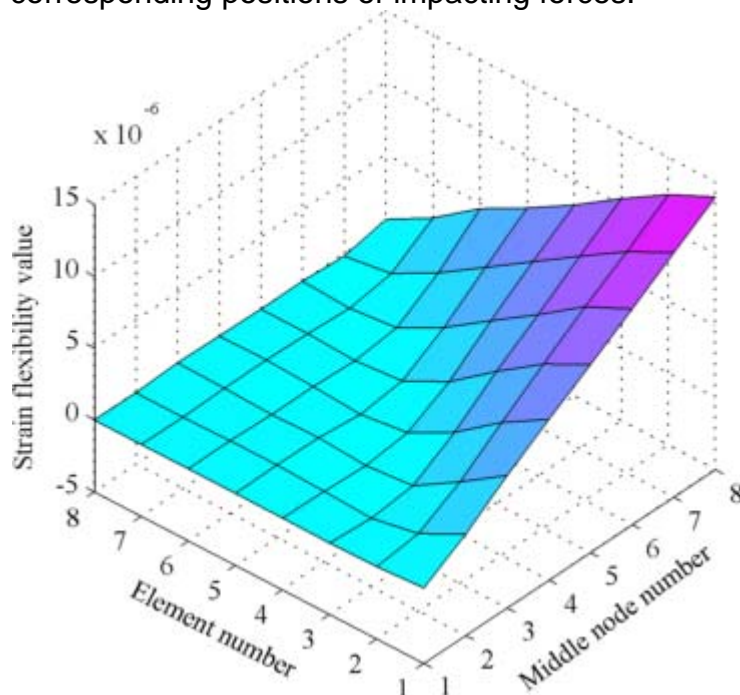


Fig. 10 Strain flexibility matrix of cantilever beam

After the strain flexibility is identified, it can be used to predict structural strain response under any static load by multiplying the load by the strain flexibility matrix. By applying contemporaneously an unitary force 1N at midpoints of 8 elements of the cantilever beam, long gauge static strain value of each element is estimated as shown in Fig. 11. It is seen that the predicted static strain values from the identified flexibility by using the first 3 modes in Eq. (20) agrees well with the static analysis results from the Sap2000 software, which successfully verified the effectiveness of the proposed method.

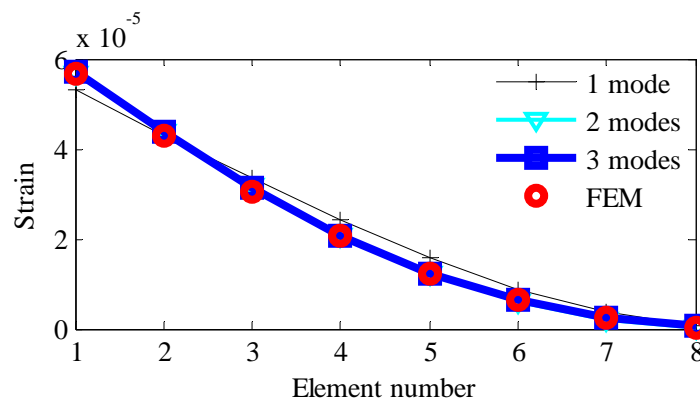


Fig. 11 Static strain prediction from the identified strain flexibility matrix

4. Conclusions

This article presents a method of structural strain flexibility identification from the multiple reference impact test data. The following conclusions can be drawn based on the research so far:

- I. Application of the long-gauge FBG sensors in SHM practices is promising owing to the fact that it has the ability of measuring both local and global information of the structure, thus it provides new opportunity for strain modal analysis theory development;
- II. The theory to identify modal parameters including frequency, strain mode shapes and displacement mode shape are developed in this article by processing the dynamic macro strain. Examples illustrated that the developed modal parameters are comparable to the exact values even in the condition that observation noise exists. Accuracy of the identified modal parameters is crucial for the strain flexibility identification. Investigation of more advanced and robust methods are further required on the basis of the results achieved in this article.

Strain flexibility identification studied in this article is seldom investigated in the literature. The success of identify structural strain flexibility is meaning for safety evaluation of structures especially for short/middle span bridges. Both displacement and strain are measured in the traditional truck load test, while the static strain can be predicted from the impact test data through the strain flexibility identification proposed in this article. Thus it is potential to carry out rapid capacity evaluation of short/middle span bridges through performing the impact test, instead of the expensive truck load test.

REFERENCES

- AASHTO 2003 Guide Manual for Condition Evaluation and LRFR of Highway Bridges (Washington, DC: AASHTO)
- Adeyuyi A. P. and Wu Z. S. (2011). "Vibration-based damage localization in flexural structures using normalized modal macrostrain techniques from limited measurements", *Computer-aided Civil and Infrastructure Engineering*. Vol. 26, No. 3, pp. 26154–26172

- Ansari, F. (1997). "Theory and applications of integrated, fiber optic sensors in structures", *Intelligent Civil Engineering Materials and Structures*, ASCE Press, Reston, Va., pp. 2–28.
- B. Peeters, G.D. Roeck. (2001). "One-year monitoring of the Z24-Bridge: environmental effects versus damage events", *Earthquake Engineering and Structural Dynamics*, Vol.30,NO.2, pp. 149-171.
- Carden, E.P., Brownjohn, J.M.W.(2008) .“Fuzzy Clustering of Stability Diagrams for Vibration-Based Structural Health Monitoring”, *Computer-Aided Civil and Infrastructure Engineering*, Vol.23,No.5,pp. 360–372.
- Casas, J.R. and Cruz, P.J.S. (2003). "Fiber optic sensors for bridge monitoring". *Journal of Bridge Engineering*, Vol.8,No.6, pp.362–373.
- D.M. Siringoringo, Y.Fujino. (2008). "System identification of suspension bridge from ambient vibration response", *Engineering Structures*, Vol.30, pp. 462-477.
- G.H. James, T.G. Carne, J.P. Lauffer. (1995). "The natural excitation technique (NEXT) for modal parameter extraction from operating structures", *The International Journal of Analytical and Experimental Modal Analysis*, Vol.10, No.4, pp. 260-277.
- H. Sohn, C.R. Farrar, F.M. Hemez, J.J. Czarnecki, D.D. Shunk, D.W. Stinemates.(2004). "A review of structural health monitoring literature: 1996-2001". *Los Alamos National Laboratory*, Report No.: LA-13976-MS.
- Hsu T. Y., Huang S. K., Lu K. C., Loh C. H., Wang Y and Lynch J.P. (2011). "On-line structural damage localization and quantification using wireless sensors", *Smart Mater Struct*. Vol.20, No.10, 5025
- Inaudi, D. (2001). Application of optical fiber sensor in civil structural monitoring. *In: Proceedings of SPIE Sensory Phenomena and Measurement Instrumentation for Smart Structures & Materials*, Newport Beach, Vol. 4328, pp. 1–10.
- J.H. Weng, C.H. Loh, J.P. Lynch, K.C Lu, P.Y. Lin, Y. Wang.(2008) . "Output-only modal identification of a cable-stayed bridge using wireless monitoring systems", *Engineering Structures*, Vol.30, No.7, pp. 1820–1830.
- J.M. Ko, Z.G Sun, Y.Q. Ni, (2002). "Multi-stage identification scheme for detecting damage in cable stayed Kap Shui Mun Bridge", *Engineering Structures*, Vol.24, No.7, pp. 857–868.
- J.M.W. Brownjohn, F. Magalhães, E. Caetano, A. Cunha, I. Au, P. Lam. (2009). Dynamic testing of the Humber Suspension Bridge, *International Conference of Experimental Vibration Analysis for Civil Engineering Structures*, Wroclaw, Poland.
- J. Zhang, J. Prader, K.A. Grimmelsman, F.L. Moon, E. Aktan, A. Shama.(2009). Challenges in Experimental Vibration Analysis for Structural Identification and Corresponding Engineering Strategies, *International Conference of Experimental Vibration Analysis for Civil Engineering Structures*, Wroclaw, Poland, 2009, pp. 13-33.
- N. Catbas, D.L. Brown, A.E. Aktan.(2004) . "Parameter estimation for multiple-input multiple-output modal analysis of large structures". *Journal of Engineering Mechanics*, Vol.130, No.8, pp. 921-30.
- Schulz, W.L., Conte, J.P. and Udd, E. (2001). "Long gage fiber optic Bragg grating strain sensors to monitor civil structures". *Proceedings of the International Society of Optical Engineering*, Vol. 4330, pp. 56–65.

- S.N. Pakzad, G.L. Fenves. (2009). "Statistical analysis of vibration modes of a suspension bridge using spatially dense wireless sensor network", *Journal of Structural Engineering*, Vol.135, No.7, pp. 863-872.
- Sohn, H., Farrar, C.R., Hemez, F.M., Shunk, D.D., Stinemates, D.W. and Nadler, B.R. (2003). A review of structural health monitoring literature: 1996–2001. *Los Alamos National Laboratory Report*, LA-13976-MS.
- S.Z.Li and Z.S.Wu. (2007). "A non-baseline algorithm for damage locating in flexural structures using dynamic distributed macro-strain responses", *Earthquake Engineering and Structural Dynamics*, Vol.36, No.9, pp. 1109-1125.
- S.Z.Li and Z.S.Wu. (2005). "Structural identification using static macro-strain measurements from fiber optic sensors", *Journal of applied mechanics*, JSCE, Vol.8, pp. 943-949.
- Udd, E. (1995). *Fiber Optic Smart Structures*, John Wiley & Sons Inc, New York.
- Yam, L.H., Leung, T.P., Li, D.B. and Xue, K.Z. (1996). "Theoretical and experimental study of modal strain energy". *Journal of Sound and Vibration*, Vol.191. No.2, pp.251–260.
- Z.S.Wu and S.Z.Li. (2006). "Two-level damage detection strategy based on modal parameters from distributed dynamic macro-strain measurements". *Journal of Intelligent Material Systems and Structures*, Vol. 18, No.7, pp. 667-676.